Cell Host & Microbe
Short Article

A Major Role for Capsule-Independent Phagocytosis-Inhibitory Mechanisms in Mammalian Infection by *Cryptococcus neoformans*

Cheryl D. Chun,[1,2] Jessica C.S. Brown,[1,2] and Hiten D. Madhani[1,*]
[1]Department of Biochemistry and Biophysics, University of California, San Francisco, 600 16th Street, San Francisco, CA 94158-2200, USA
[2]These authors contributed equally to this work
*Correspondence: hitenmadhani@gmail.com
DOI 10.1016/j.chom.2011.02.003

SUMMARY

The antiphagocytic polysaccharide capsule of the human fungal pathogen *Cryptococcus neoformans* is a major virulence attribute. However, previous studies of the pleiotropic virulence determinant Gat201, a GATA family transcription factor, suggested that capsule-independent antiphagocytic mechanisms exist. We have determined that Gat201 controls the mRNA levels of ~1100 genes (16% of the genome) and binds the upstream regions of ~130 genes. Seven Gat201-bound genes encode for putative and known transcription factors—including two previously implicated in virulence—suggesting an extensive regulatory network. Systematic analysis pinpointed two critical Gat201-bound genes, *GAT204* (a transcription factor) and *BLP1*, which account for much of the capsule-independent antiphagocytic function of Gat201. A strong correlation was observed between the quantitative effects of single and double mutants on phagocytosis in vitro and on host colonization in vivo. This genetic dissection provides evidence that capsule-independent antiphagocytic mechanisms are pivotal for successful mammalian infection by *C. neoformans*.

INTRODUCTION

The fungus *Cryptococcus neoformans* is a leading cause of morbidity and mortality in AIDS patients, resulting in one million cases and 600,000 deaths annually worldwide (Park et al., 2009). Although cryptococcosis is typically associated with immunodeficient patients, a recent outbreak caused by the sister species *Cryptococcus gattii* in the Pacific Northwest has resulted in the deaths of numerous immunocompetent individuals (Datta et al., 2009). It is thus critical to understand the interactions of the *Cryptococcus* species complex with the mammalian immune system.

C. neoformans is thought to be acquired through the inhalation of spores or yeast (Botts and Hull, 2010), and alveolar macrophages are considered the first line of defense against cryptococcal infection. Experimental evidence supports this, particularly early in infection (Monga, 1981; Osterholzer et al., 2009). *C. neoformans* can also survive and proliferate within the phagolysosome, as well as exit macrophages by lytic and nonlytic pathways, all of which might be important for pathogenesis (Voelz and May, 2010). Macrophage activation has been shown to be important for T cell proliferation, the development of the T cell response, and chemokine-mediated recruitment of neutrophils and monocytes into the tissue (Monari et al., 2006a).

C. neoformans is rarely taken up by macrophages in the absence of opsonizing agents such as complement or antibodies, even after 24 hr of coincubation (Levitz and DiBenedetto, 1989; Liu et al., 2008). This is in striking contrast to other yeasts: unopsonized *Saccharomyces cerevisiae* or *Candida albicans* are phagocytosed after less than 1 hr of coincubation (Lohse and Johnson, 2008; Tejle et al., 2002). Opsonizing agents are likely to be present in lower levels early in infection. Within the lungs, complement is not present at constitutively high levels, but is synthesized in response to infection by many different cell types within the lungs and other tissues in a process that is estimated to take up to 1 week (Blackstock and Murphy, 1997; Rothman et al., 1989). Antibody generation is thought to take 2 to 5 weeks for peak production (Nussbaum et al., 1999). Therefore, cell-mediated killing by macrophages during the initial infection, prior to complement and antibody generation, is likely to be important for limiting proliferation of the invading pathogen. Studies have shown that AIDS patients generate less anti-*C. neoformans* antibody than healthy patients, and the severe prognosis for cryptococcosis in AIDS patients may be linked to this defect (Subramaniam et al., 2009). Antibodies generated by infected AIDS patients may be less protective against *C. neoformans* infection or produced at titers too low for effective opsonization, or production could be critically delayed early in infection (Dromer et al., 1988, 1995). It is thus possible that yeast evasion of phagocytosis by macrophages plays an important role in the development of cryptococcosis in immunocompromised individuals.

The characteristic polysaccharide capsule of *C. neoformans* is considered one of its chief virulence traits. Its primary components are glucuronoxylomannan (GXM) and galactoxylomannan (GalXM), two high-molecular-mass polymers that have immunomodulatory properties, including suppression of both adaptive and innate immune mechanisms (Monari et al., 2006a, 2006b) The production of capsule by *C. neoformans* has been previously associated with inhibition of phagocytosis, although this correlation has been reported predominantly in the context of *C. neoformans* cells opsonized with serum (Del Poeta, 2004). It remains

unclear how the capsular polysaccharides GXM and GalXM contribute to inhibition of unopsonized phagocytosis, which is presumably relevant to the control of disease early in the infection process. While the capsule is clearly an important virulence trait, clinical studies have suggested for decades the existence of important capsule-independent mechanisms: cryptococcosis cases produced by capsule-deficient strains exhibit a similar clinical course as infections produced by capsule-proficient strains (Torres et al., 2005).

Previously, our group described the first large-scale systematic genetic screen for virulence determinants of *C. neoformans* (Liu et al., 2008). We constructed and analyzed ~1200 gene knockout strains in the background of the H99 clinical isolate of *C. neoformans var grubii* (serotype A). A signature-tagged mutagenesis screen led to the identification of numerous factors required for the expression of known virulence factors, as well as dozens of genes that contributed to virulence independently of known mechanisms. Among the mutants that produced the strongest defect in infectivity but did not affect proliferation rate at body temperature was a deletion in the *GAT201* gene (Liu et al., 2008). *GAT201* encodes a member of the GATA family of zinc-finger transcriptional regulators that is conserved from yeast to man (Teakle and Gilmartin, 1998). A *GAT201* knockout mutant shows reduced capsule size and dramatic attenuation in virulence in a mouse inhalation model of infection. Significantly, we found that *gat201Δ* mutants are robustly taken up by macrophages in unopsonized conditions. In contrast, less than 1% of macrophages are associated with yeast when infected with wild-type *C. neoformans* for the same period. The defect in phagocytosis evasion by *gat201*Δ cells cannot be explained by the capsule size defect exhibited by *gat201*Δ cells: *cap10*Δ, *cap60*Δ, and *cap64*Δ cells, which are devoid of capsule, display a much more modest increase in association with macrophages than a *gat201*Δ mutant. More importantly, when *CAP* genes are knocked out in combination with *GAT201*, the resulting *capΔgat201*Δ strains still show dramatically increased percentages of macrophages with associated yeast cells over that displayed by the single *cap* mutants. These data suggested that Gat201 inhibits phagocytosis via both capsule-dependent and capsule-independent mechanisms (Liu et al., 2008). However, the relative contribution of these two functions to the virulence function of Gat201 remained to be addressed.

Given that Gat201 is predicted to be a transcriptional regulator, understanding its role in virulence requires identification and characterization of its direct targets. Chromatin immunoprecipitation-microarray hybridization (ChIP-chip) and chromatin immunoprecipitation sequencing (ChIP-seq) are ideal methods for identifying direct targets of transcription factors, but the application of these methods to *C. neoformans* (whose polysaccharide capsule thickness can exceed the diameter of the cell) is nontrivial. In this study, we report the successful development of ChIP-chip methods for capsule-bearing *C. neoformans*, the identification of the direct targets of Gat201, and detailed analysis of these targets by systematic gene disruption and phenotypic characterization. We demonstrate that two targets, *GAT204* and *BLP1*, together explain a bulk of the capsule-independent phagocytosis evasion (''antiphagocytosis'') activity of Gat201 and that they are critical for *C. neoformans*'s ability to colonize the mammalian lung early in the infection process.

RESULTS

Gat201 Controls the Expression of ~1100 Genes in Response to Environmental Cues

Our previous work (Liu et al., 2008) indicated that Gat201 is a key virulence regulator, possibly through its inhibition of phagocytosis by macrophages. As Gat201 is a GATA family transcription factor, we used microarray-based expression profiling to identify genes that are transcriptionally regulated by Gat201 (Figure 1A). When we compared the transcript profiles of wild-type cells to *gat201Δ* cells grown in standard yeast culture conditions (30°C, YPAD medium, atmospheric CO_2), we observed few changes in messenger RNA (mRNA) accumulation as determined with statistical analysis of microarrays (SAM) analysis (Tusher et al., 2001). In comparison, when the strains were cultured in tissue culture conditions (37°C, Dulbecco's modified Eagle's medium [DMEM], 5% CO_2), the same conditions used for culturing macrophages, we saw a dramatic Gat201-dependent transcriptional program (Figure 1B). Over 1100 genes (~16% of the genome) showed a ≥2-fold difference in transcript levels and were identified by SAM analysis as differentially up- or downregulated in a Gat201-dependent manner. We performed time course experiments utilizing RT-qPCR to examine gene expression of two representative genes from the upregulated set (*MEU1* and *CNJ1810*) after transfer of cells from yeast to tissue culture conditions. Through the time course, we observed steady increases in transcript levels, with maximal expression occurring between 8 and 24 hr after transfer (Figure 1C). Interestingly, *GAT201* RNA levels also increased dramatically under these conditions, suggesting a positive feedback loop.

Gat201 Binds the Promoters of 126 Genes and Controls mRNA Levels of 62 of These Genes

To identify genes directly bound by Gat201, we used a ChIP-chip approach (Nobile et al., 2009). We tagged the endogenous *GAT201* gene with a C-terminal calmodulin-binding peptide-2X FLAG (CBP-2XFLAG) epitope. For these studies, we developed a ChIP protocol for encapsulated cells (see the Supplemental Experimental Procedures). Immunoprecipitated DNA (IP) and reference DNA (WCE) from a Gat201-CBP-2XFLAG-expressing and an untagged parent strain were amplified and hybridized against a custom microarray spanning the entire genome of the strain H99. We identified 126 genes that show enrichment of Gat201-CBP-2XFLAG in their promoter regions when compared to the reference DNA and the untagged control strain (Figure 1D). As predicted from our time course analysis, Gat201-CBP-2XFLAG binds in the promoter of *GAT201* itself (Figure 1E).

Having identified genes with Gat201-CBP-2XFLAG bound in their promoters, we next sought to determine whether their transcription was Gat201-dependent (Figure S1 available online). We used RT-qPCR to quantify the mRNA levels for 126 genes with the strongest enrichment for Gat201-CBP-2XFLAG in their promoters, comparing wild-type and *gat201Δ* cells grown in yeast culture and tissue culture conditions. Transcript levels were normalized to the levels found in wild-type cells grown in yeast culture conditions. We identified a set of 62 Gat201-bound genes that demonstrated Gat201-dependent transcription induction in tissue culture conditions (Table 1). The promoter regions of these genes are enriched for a 7 nt motif when

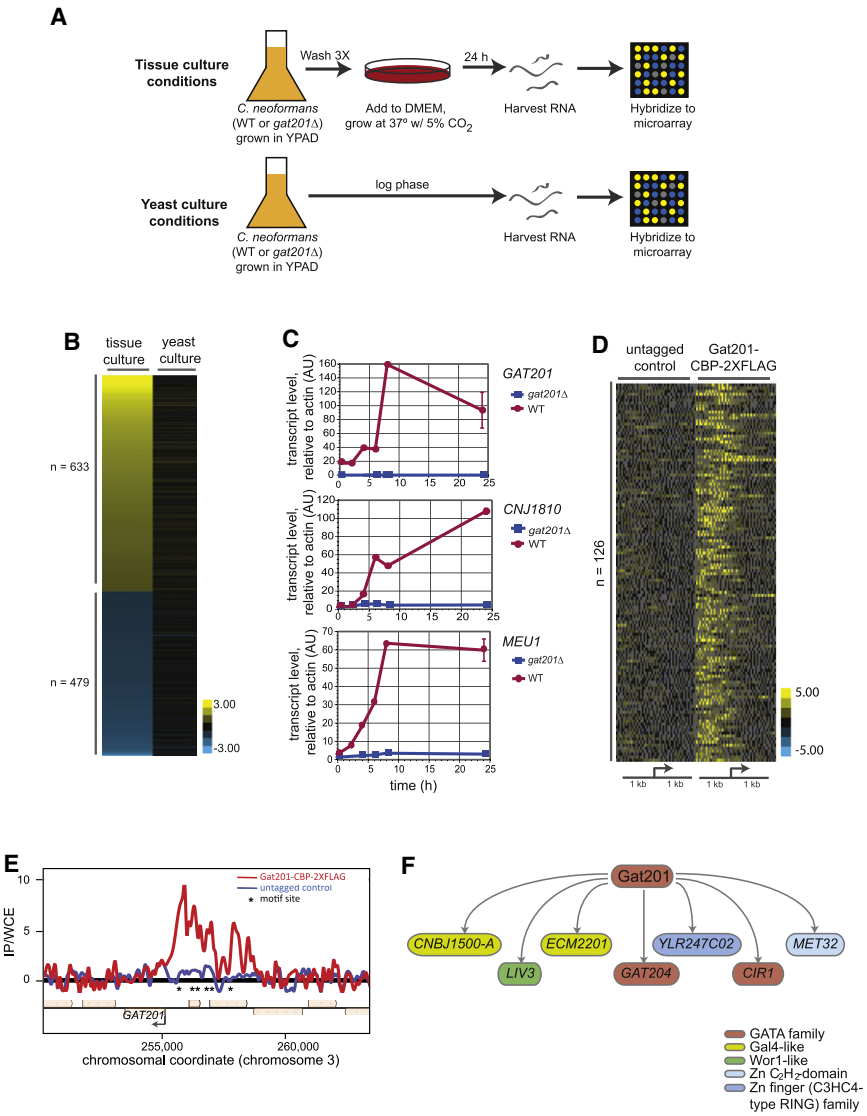

Figure 1. Identification of Gat201 Transcriptional Program and Direct Gat201 Targets

(A) Schematic of growth conditions used for transcriptional microarrays of yeast cells grown in tissue culture conditions (DMEM, 37°C, 5% CO_2) or yeast culture conditions (YPAD, 30°C, atmospheric CO_2).

(B) Transcript profiling with custom whole-genome DNA microarrays was performed comparing *gat201Δ* versus wild-type cells grown in tissue culture and in yeast culture conditions. Genes shown are those with both a minimum of a 2-fold change and a statistically significant difference (with SAM analysis) between expression profiles in tissue culture and yeast media conditions. Values are plotted as the average ratio of transcript level in *gat201Δ* cells versus wild-type cells (log_2) from four arrays per growth condition.

(C) RT-qPCR analysis of the indicated transcripts after transfer from yeast culture conditions into tissue culture conditions. Samples were harvested at the indicated time points after transfer for RNA isolation and complementary DNA synthesis. Error bars at the 24 hr time point are the standard deviation of two samples.

(D) Global summary of ChIP-chip results. Genes enriched for Gat201-CBP-2XFLAG bound in their promoter regions were identified by comparing signals from replicate experiments performed with untagged and tagged strains. Genes displayed are those with the largest difference between tagged and untagged genotypes in median value of the top five probe values among those within 1 kb of the predicted translational start site. Depicted are the ratios (log_2) of immunoprecipitated DNA (IP) to whole-cell extract (WCE) for each probe.

(E) Example of ChIP-chip data. Ratios (log_2) of IP DNA to WCE were plotted for each probe of the two tiling arrays at the chromosomal coordinates indicated. Asterisks indicate locations of motif in the chromosomal sequence shown.

(F) Gat201 directly binds the regulatory regions of set of known and putative transcription factors.

See also Figure S2.

compared to the promoters of all genes in the H99 *C. neoformans* genome (Figure S2A). Strikingly, Gat201 activates the transcription of genes encoding seven known and putative transcription factors: *CNBJ1500-A*, *GAT204*, *ECM2201*, *CIR1*, *LIV3*, *YLR236C02*, and *MET32*. These results suggest that Gat201 controls its remarkably large transcriptional regulon in part by activating the transcription of genes coding for downstream regulators (Figure 1F).

Identification of Key Gat201-Bound Genes

We considered the 62 direct downstream targets of Gat201 to be likely effectors of Gat201-mediated phagocytosis inhibition. We thus targeted each of these genes for deletion by homologous recombination (Figure S1A). We successfully knocked out 46 of 62 genes and then tested each of the mutant strains for phagocytosis defects by coincubation with RAW264.7 macrophages. Two genes emerged as having a role in phagocytosis inhibition: *CNAG_06346* and *CNAG_06762*. *CNAG_06346* encodes a protein with a highly conserved Barwin-like domain that we named *B*arwin-*l*ike *p*rotein 1 (Blp1). *CNAG_06762* encodes for the GATA family transcription factor that we previously annotated as Gat204 (Chow et al., 2007). *BLP1* and *GAT204* show enhanced binding of Gat201-CBP-2XFLAG in their promoter regions (Figure S2B), and their expression is Gat201-dependent in tissue culture conditions (Figure 2A).

As Gat204 is itself a transcription factor, we examined *BLP1* transcription in *gat204Δ* cells. *BLP1* expression is increased in *gat204Δ* cells in tissue culture conditions (Figure 2B), suggesting that Gat204 may negatively regulate *BLP1* transcription or that *BLP1* transcription is upregulated as a compensatory mechanism when Gat204 is lost.

Gat201-Bound Genes Mediate Its Antiphagocytic Function

After 24 hr coincubation with *blp1Δ* cells, approximately 2.5% of RAW264.7 macrophages were associated with yeast, a modest

Table 1. Gat201 Target Genes

CNAG Number	CDS Number	WT/*gat201Δ*	DMEM Induction	Name	Annotation
CNAG_06517	CDS_4922	144.51	117.50	YOR296W02	C2 domain-containing protein
CNAG_04736	CDS_5892	103.76	153.95	CNJ1800	unknown
CNAG_06186	CDS_1099	37.53	103.95	CNM1740	sugar transport
CNAG_01553	CDS_3244	35.87	36.20	CNC0890	CHORD-containing protein
CNAG_05867	CDS_3724	32.25	239.48	CNF3650	fucose permease
CNAG_01601	*CDS_2811*	*31.95*	*195.53*	*ATG15*	*potential vacuolar triglyceride lipase*
CNAG_06389	CDS_7034	31.10	20.86	–	unknown
CNAG_05147	CDS_5668	23.64	51.11	CNI2090	unknown
CNAG_04735	CDS_5889	23.00	69.96	CNJ1810	metalloprotease
CNAG_00165	CDS_4036	18.59	39.71	MEU1	phosphorylase
CNAG_04756	CDS_5770	15.69	72.05	CNJ1610	ribonuclease H-related protein
CNAG_00331	*CDS_4152*	*8.49*	*22.77*	*YMR210W01*	*alpha/beta hydrolase fold*
CNAG_02553	*CDS_1762*	*8.31*	*17.90*	*SPS1904*	*putative oxidoreductase*
CNAG_05821	*ND*	*8.20*	*20.59*	–	*unknown*
CNAG_03848	CDS_6469	8.07	22.97	CNB2310-B	putative glutaredoxin
CNAG_05312	CDS_5280	7.93	3.45	CNI3590	macrophage-activating glycoprotein
CNAG_00456	*ND*	*6.93*	*24.06*	–	*unknown*
CNAG_00374	CDS_6603	6.27	10.73	–	unknown
CNAG_01777	CDS_2931	6.19	1.47	YNL274C03	glyoxylate reductase
CNAG_00919	*CDS_669*	*5.67*	*3.05*	*KEX101*	*carboxypeptidase S3*
CNAG_06762	CDS_5944	5.57	36.16	GAT204	GATA family transcription factor
CNAG_01552	*CDS_3426*	*5.38*	*44.66*	*BET1*	*T-SNARE membrane protein*
CNAG_06346	ND	5.04	5.14	BLP1	Barwin-like domain
CNAG_05640	CDS_5612	5.02	7.19	SMF1	NRAMP manganese transporter
CNAG_06493	CDS_4944	4.81	14.99	CNN2220	unknown
CNAG_02189	CDS_1614	4.68	7.46	YJL216C	putative alpha amylase
CNAG_03012	*CDS_2777*	*4.52*	*2.07*	*QSP1*	*quorum-sensing peptide*
CNAG_02777	CDS_3007	4.49	158.67	PHO840	putative phosphate transporter
CNAG_05664	CDS_5254	2.17	1.22	BAT1	branched amino acid transaminase
CNAG_03136	CDS_2688	4.29	20.43	CNG0410	putative fatty acid synthase
CNAG_04768	*CDS_5907*	*4.14*	*6.35*	*CNBJ1500-A*	*Gal4-like DNA binding domain*
CNAG_06098	CDS_1286	4.09	5.40	CNM0910	glucosamine-6-phosphate
CNAG_03122	ND	3.82	772.37	–	unknown
CNAG_06200	CDS_1088	3.70	3.92	CNM1860	PAS domain-containing protein
CNAG_06242	CDS_1107	3.56	8.20	CFT1	high-affinity iron permease
CNAG_06108	ND	3.40	2.83	–	unknown
CNAG_01778	*CDS_3364*	*3.30*	*6.15*	*CNC4450*	*mitochondrial carrier protein-like*
CNAG_04737	CDS_5893	3.25	1.50	CNJ1790	potential methyltransferase
CNAG_04517	ND	3.21	3.64	–	unknown
CNAG_00883	CDS_781	3.00	11.16	ECM2201	Gal4-like DNA binding
CNAG_05229	CDS_5329	2.86	19.11	CNI2770	stomatin-like protein
CNAG_00884	CDS_775	2.74	5.74	SEC10	unknown
CNAG_03413	CDS_2415	2.73	9.52	CNG3070	alginate lyase
CNAG_04312	*CDS_112*	*2.43*	*2.88*	*PMI4001*	*mannose-6-phosphate isomerase*
CNAG_05835	CDS_3521	2.35	3.21	LIV3	Wor1-like transcription factor
CNAG_03915	CDS_6280	2.32	9.78	CNB1700	unknown
CNAG_04140	CDS_43	2.20	4.99	CNH2650	unknown
CNAG_02856	*CDS_3358*	*2.20*	*2.05*	*TRK1*	*putative potassium transporter*
CNAG_03412	CDS_2417	2.16	3.97	CTS202	chitinase
CNAG_02219	CDS_1876	2.08	1.71	YLR247C02	zinc finger

Table 1. *Continued*

CNAG Number	CDS Number	WT/*gat201Δ*	DMEM Induction	Name	Annotation
CNAG_03847	CDS_6346	2.08	7.85	CNB2320	unknown
CNAG_01681	CDS_2877	2.07	10.13	FCY2201	putative purine-cytosine permease
CNAG_06763	CDS_5942	2.05	6.61	DIA4	putative seryl-tRNA synthetase
CNAG_04864	CDS_5991	2.01	3.22	CIR1	GATA-type transcription factor
CNAG_04436	CDS_146	1.99	12.71	CNH1150	unknown
CNAG_04435	*ND*	*1.97*	*6.83*	–	*ferric reductase*
CNAG_00184	CDS_4067	1.84	1.87	PCF11	Pre-mRNA cleavage complex II
CNAG_00068	CDS_4631	1.81	7.46	MET32	Zn C2H2-domain containing protein
CNAG_06187	ND	2.54	3.39	STR1	streptomycin biosynthesis protein
CNAG_01040	CDS_703	24.63	10.64	KEX102	carboxypeptidase S3
CNAG_05159	*ND*	*18.83*	*6.09*	–	*unknown*
CNAG_00546	*CDS_4340*	*2.95*	*5.68*	*CHS301*	*chitin synthase*

Genes with Gat201-CBP-2XFLAG bound in their promoter with Gat201-dependent induction in tissue culture conditions. CNAG numbers are gene identifiers from the Broad Institute's annotation of H99. CDS numbers are gene identifiers from our annotation. "WT/*gat201Δ*" refers to the ratio of transcript level for a given gene in wild-type cells over that in *gat201Δ* cells in tissue culture conditions. "DMEM induction" is the amount of transcript for a given gene in wild-type cells grown in tissue culture conditions relative to the transcript level in wild-type cells grown in yeast culture conditions. When previously characterized in the literature, the name for a gene is given. If there is no prior reference to the gene, the name assigned in our annotation is given, if available. Annotations were assigned by BLASTP and SMART analysis. Italics indicate those genes that were not successfully knocked out.

but statistically significant ($p < 0.05$) increase over the 0.8% of macrophages associated with wild-type yeast (Figure 2C). Coincubation with *gat204Δ* cells resulted in yeast association in ~9% of RAW264.7 cells. Strikingly, two independently-derived double-knockout strains in *GAT204* and *BLP1* showed 25%–30% of RAW264.7 macrophages associated with *C. neoformans*, indicating a functional synergy in their mechanism of phagocytosis inhibition, and recapitulating almost 40% of the original Gat201-dependent phenotype. We also observed this synergistic increase in phagocytosis in bone marrow-derived macrophages (BMDMs) (Figure S3A). Finally, we distinguished between macrophage-internalized and -externally associated yeast cells using differential staining techniques. We confirmed that the *gat204Δ* and *blp1Δ* mutations acted synergistically to produce increases in actual uptake. We also documented an increase in external association of *gat204*Δ, *blp1*Δ, and *gat204*Δ*blp1*Δ strains (Figures S3B and S3C), which suggests that recognition and adherence may be what is triggering phagocytosis in the mutants.

Agrobacterium Transfer DNA Insertion Screen Independently Identifies *GAT201* and *GAT204*

Our original knockout library only covered a portion of the *C. neoformans* genome, so we sought a more global approach to identify anti-phagocytic factors. We therefore used the *Agrobacterium tumefaciens* transfer DNA system (McClelland et al., 2005) to produce insertional mutants across the *C. neoformans* genome and then screened this mutant library for anti-phagocytosic defects (Figure S1B). A library of ~30,000 insertions was generated, from which 2×10^8 yeast cells from overnight YPAD culture were added to plated RAW264.7 macrophages. After rounds of selection for phagocytosed yeast cells, the yeast culture was enriched for strains mutated in genes important for phagocytosis inhibition. The sites of insertion were mapped for strains that individually demonstrated increased uptake by macrophages. Strikingly, this global approach identified three independent insertional events each into *GAT201* and *GAT204* (Figure S1C). We also identified the copper transporter *CTR2*, a gene not regulated by Gat201 that causes capsule defects when mutated and is thus presented elsewhere (Chun and Madhani, 2010). We did not identify strains with mutations in *BLP1* in this screen, which is not surprising given the mild phenotype of the *blp1Δ* single mutant. We also did not identify capsule gene mutants; however, these strains exhibit a growth defect (C.D.C. and H.D.M., unpublished data) and are likely outcompeted during the selection process. Another gene known to be involved in capsule-independent phagocytosis, *APP1*, acts only in opsonized cells (Luberto et al., 2003) and was not identified in our screen for unopsonized phagocytosis. These data underline the importance of Gat201 and Gat204 in limiting phagocytosis of *C. neoformans*.

Gat204 and Blp1 Are Dispensable for Capsule Formation

Interestingly, the level of capsule, as detected by India ink staining (Figure 2D), was unchanged in these mutants, unlike in the *gat201Δ* strain (Liu et al., 2008). *gat204*Δ, *blp1*Δ, and *gat204*Δ*blp1*Δ mutants were also stained for β-glucan, chitin, and mannoprotein but did not show any changes relative to wild-type cells (data not shown), demonstrating that gross cell surface architecture is unchanged in these mutants. Growth at 37°C was unchanged in the *gat204*Δ and *blp1*Δ mutant strains (Figure 3A). None of the mutants were deficient in the production of melanin, a pigmented compound thought to be important for virulence in the host (Figure 3B).

Blp1 Is Part of a Six-Gene Family in *C. neoformans*

SMART protein sequence analysis of Blp1 identified a conserved Barwin-like domain (Figure S2C). This domain is found in a number of protein families in plants, fungi, and bacteria, several members of which have antifungal properties (Hejgaard et al.,

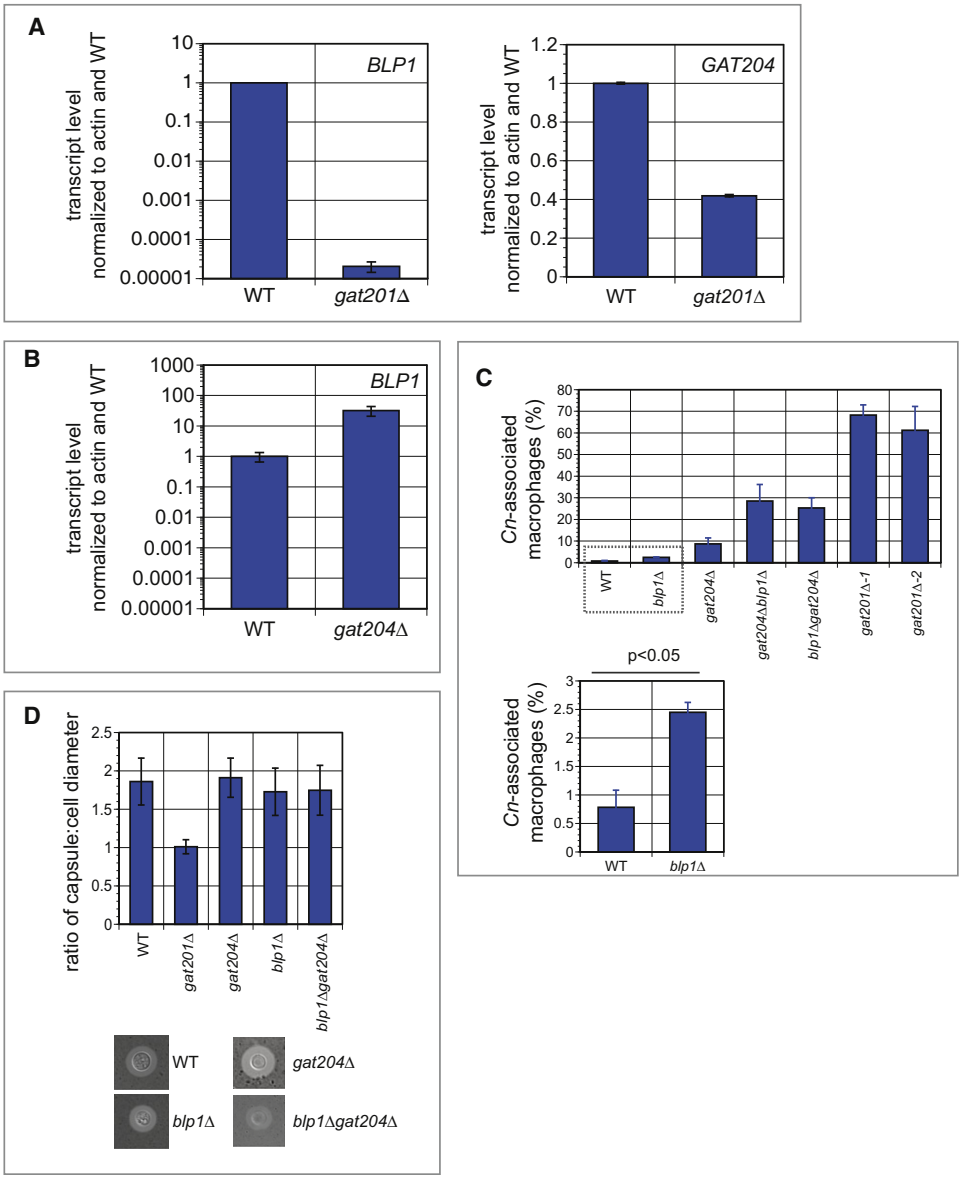

Figure 2. In Vitro Analysis of Gat204 and Blp1

(A) Activation of *BLP1* and *GAT204* by Gat201. *BLP1* (left) and *GAT204* (right) transcript levels were assessed in wild-type and *gat201Δ* cells grown in tissue culture conditions for 24 hr. Error bars are standard deviation (SD) of two to four samples.

(B) Repression of *BLP1* by Gat204. *BLP1* transcript levels were assessed in wild-type and *gat204Δ* cells grown in tissue culture conditions for 24 hr. Error bars are SD of two samples.

(C) Quantification of phagocytosis defects. RAW264.7 macrophages were coincubated with the designated *C. neoformans* strains for 24 hr then washed three times with PBS to remove unphagocytosed yeast. The macrophages were then counted to assay the number of macrophages with yeast associated. At least 200 macrophages were counted per well, and each strain was assayed in triplicate. By Student's t test, the difference between *blp1Δ* and wild-type association with macrophages was determined to be statistically significant.

(D) Quantitative measurements of capsule size. Capsule was induced in the indicated strains by incubation in tissue culture conditions for 24 hr. Capsule and cell size were measured for at least 30 cells per strain, and the ratio of capsule to cell diameter calculated and averaged for each strain. Error bars represent the standard deviation (SD).

See also Figure S1.

1992). Analysis of predicted protein sequence by SignalP reveals a high probability (1.000) of a signal peptide. *BLP1* appears to be part of a six-member family in *C. neoformans*, all members of which contain the Barwin-like domain and a signal sequence.

Inhibition of Phagocytosis Correlates with Effective Colonization of the Lungs

To determine whether inhibition of phagocytosis by *C. neoformans* correlates with its ability to colonize the lung, we

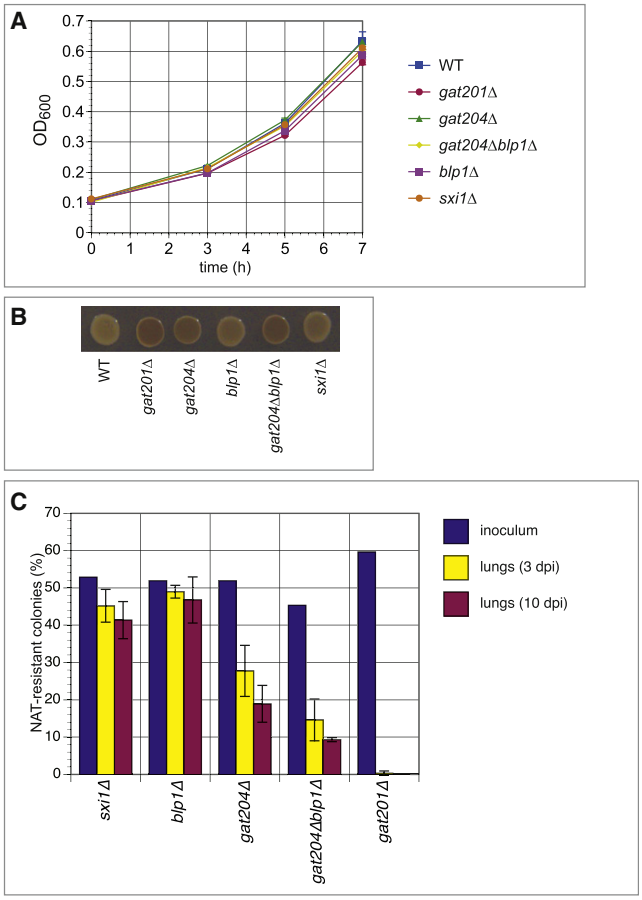

Figure 3. Antiphagocytosis Mutants Show Reduced Fitness during Infection but Normal Rates In Vitro

(A) Growth rate measurements. Log-phase wild-type and mutant strains were grown for 7 hours at 37°C in YPAD medium, and OD_{600} was measured every 2–3 hr. Error bars represent the SD for cultures grown in triplicate.

(B) Melanin assays. Melanin assay on L-DOPA plates demonstrates that none of the strains are hypomelanized. *gat201Δ* is hypermelanized, as previously noted in Liu et al. (2008). *gat204Δ* is also hypermelanized, as is the *gat204Δblp1Δ* mutant.

(C) Mouse infection data. Approximately 1:1 mixtures of H99 and the indicated mutant (marked with a nourseothricin [NAT] resistance gene) were inoculated intranasally into mice (A/J) (5×10^5 total cells/mouse). The actual proportion of mutant cells in each inoculum were determined by plating of a dilution of the inoculum on nonselective medium and then assaying of 100–200 individual colonies for NAT resistance. At 3 and 10 days after infection, animals were sacrificed, and the lungs, brains, and spleen from each were homogenized and serial dilutions were plated. One hundred to 200 colonies per organ were assayed for NAT resistance to determine the percentage of mutant cells. Error bars represent the SD from three mice per inoculum.

See also Figure S3.

performed competitive infections. Wild-type cells were mixed in equal proportion with *gat201Δ*, *gat204Δ*, *blp1Δ*, or *gat204Δblp1*Δ cells. As a control strain, we used a knockout mutant in *SXI1*, which is not expressed in nonmating cells and is dispensable for virulence (Hull et al., 2004). Inocula were administered to mice through an inhalation model of infection. The lungs were harvested after 3 or 10 days, and the proportion of mutant to wild-type cells was assessed. Strikingly, we observed a correlation between the degree of phagocytosis inhibition in a given strain and the relative ability of that strain to colonize the lung tissue (Figure 3C). While the mutant cells made up ~50% of each inoculum, their prevalence after 3 or 10 days in the lungs correlated with their antiphagocytic abilities. The *gat201Δ* strain, which showed the least phagocytic inhibition of all the strains tested, was entirely absent from lung tissue homogenate-derived colonies. The *gat204Δ* strain, which showed decreased phagocytic inhibition compared to the wild-type, also displayed decreased representation in the lungs (~27% at 3 dpi, ~19% at 10 dpi). *gat204Δblp1Δ*, which displayed a level of phagocytic inhibition between that of *gat201Δ* and *gat204Δ*, showed a level of representation in the lungs also intermediate to the two strains. The *blp1Δ* mutant, which displayed the weakest phagocytosis phenotype, and the control *sxi1Δ* mutant represented ~50% of the cells recovered from the lungs.

DISCUSSION

Cryptococcus species produce a polysaccharide capsule, which numerous studies have shown to be a major virulence factor and an important mechanism of immune modulation. In particular, capsule inhibits phagocytosis of *C. neoformans* by macrophages (Monari et al., 2006a). However, our previous work demonstrates that the pleiotropic transcriptional activator Gat201 controls a capsule-independent mechanism by which *C. neoformans* evades phagocytosis but also regulates capsule synthesis (Liu et al., 2008). Here, we describe a regulatory circuit dissection approach to further illuminate capsule-independent antiphagocytic mechanisms and to test their roles in infection. The work described in this paper demonstrates that at least two such mechanisms exist, begins to identify potential end effectors of this regulatory circuit, and—importantly—provides strong evidence that such mechanisms are important for successful mammalian infection by *C. neoformans*.

An Integrative Approach Identifies the Direct Targets of the Gat201 Virulence Regulator

We found that over 1000 genes, or approximately one-sixth of the *C. neoformans* genome, showed statistically significant changes in expression in *gat201Δ* cells compared to the wild-type. As expression of *GAT201* itself was induced in these conditions, Gat201 could function downstream of a signaling pathway(s) that senses environmental changes and modulates a massive reprogramming of the cellular transcriptome.

To identify the direct targets of Gat201, we developed ChIP-chip methods. Through this approach, we identified 126 genes that demonstrate robust binding of Gat201 in their promoter regions, 62 of which depend on Gat201 for transcript accumulation in tissue culture conditions. Significantly, seven targets of Gat201 themselves encode known or predicted transcription factors, two of which, Liv3 and Cir1, have been previously implicated in pathogenicity (Jung et al., 2006; Liu et al., 2008). The results reported here implicate Gat204 in infectivity. Thus, it appears that Gat201 is part of a critical large virulence transcriptional regulatory network that controls pathogenicity in response to environmental signals.

Systematic Analysis Reveals the Existence of Multiple Capsule-Independent Antiphagocytosis Mechanisms

Through a systematic gene disruption approach, we identified two genes, *BLP1* and *GAT204*, which affect the ability of *C. neoformans* to evade unopsonized phagocytosis by macrophages. Together, these two genes recapitulate a significant portion of the phenotype of the *gat201*Δ mutant strain. These observations suggest that at least three mechanisms exist to inhibit phagocytosis: GXM, those dependent on Blp1 and Gat204, and at least one mechanism that is Gat201 dependent but Blp1/Gat204 independent.

Capsule-Independent Phagocytosis Inhibition and Mammalian Infectivity of *Cryptococcus neoformans*

Finally, we have demonstrated that the relative ability of a given strain to evade or inhibit phagocytosis correlates with its ability to survive and proliferate within the lung tissue. We examined time points relatively early in infection, when we expect alveolar macrophages to play a crucial role in the initial host response, but before a full adaptive immune response develops. Cells lacking Gat201 are cleared from the lungs of infected mice within 3 days, demonstrating an early and pivotal role for this transcription factor in pathogen success. Significantly, the analysis of single and double mutants demonstrated that the roles of Gat201, Gat204, and Blp1 in survival within the murine lung are proportional to their impact on phagocytosis in vitro. The correlation between the in vitro and in vivo data strongly indicates that multiple capsule-independent antiphagocytosis mechanisms are critical for infection of the mammalian host. Thus, while a major focus of *C. neoformans* research has justifiably been its polysaccharide capsule, this work demonstrates capsule-independent antiphagocytic mechanisms are important for successful host colonization.

EXPERIMENTAL PROCEDURES

Gene Nomenclature

Genes were identified with annotation from the H99 sequence from the Broad Institute (http://www.broadinstitute.org/annotation/genome/cryptococcus_neoformans/MultiHome.html) and from our own annotation of the H99 sequence (http://cryptogenome.ucsf.edu/). Gene annotations from the Broad Institute are designated by the nomenclature "CNAG_#," while our own annotations are designated "CDS_#."

Strains and Media

C. neoformans growth conditions were as previously described (Chun et al., 2007; Chun and Madhani, 2010; Liu et al., 2008), with minor modifications found in the Supplemental Experimental Procedures.

Phagocytois Assay

RAW264.7 macrophage assays were performed as previously described (Chun and Madhani, 2010; Liu et al., 2008). Bone marrow-derived macrophage experiments were performed in much the same manner with minor modifications described in the Supplemental Experimental Procedures.

Expression Profiling

Expression profiling was performed as previously described (Liu et al., 2008) with minor modifications described in the Supplemental Experimental Procedures. Analysis was performed as described in Chun et al. (2007).

ChIP-chip

The ChIP-chip tiling arrays were designed on 244,000 probes of 60 bp length, averaging 80 bp between probes, across the entire H99 sequence as it was published by the Broad Institute, current to 2007. Experiments were performed as previously described (Nobile et al., 2009) with *C. neoformans*-specific modifications described in the Supplemental Experimental Procedures.

RT-qPCR

Gene expression differences observed using microarray-based transcript profiling were confirmed utilizing RT-qPCR as previously described (Chun et al., 2007) with minor modifications (see the Supplemental Experimental Procedures).

A. tumefaciens-Mediated Transformation of *C. neoformans*

These experiments were performed as described in McClelland et al. (2005) with minor modifications as described in Chun and Madhani (2010).

Phagocytosis Screen with Insertional Mutant Library

This procedure was performed as previously described (Chun and Madhani, 2010).

Capsule Assay

Experiments were performed as previously described (Liu et al., 2008). See the Supplemental Experimental Procedures for more details.

Growth Curve

Overnight YPAD cultures grown at 37°C were diluted back to OD_{600} = 0.1 in YPAD, in triplicate. Cultures were grown at 37°C for 7 hr, and the OD_{600} was measured every 2–3 hr.

Melanin Assay

From overnight culture, *C. neoformans* cells were diluted to OD_{600} = 0.6 in water then spotted onto melanin-inducing plates containing L-DOPA (L-dihydroxyphenylalanine, Sigma, 100 mg l^{-1}) and grown for 3 days at 37°C.

Intranasal Coinfection Experiments

Experiments were performed as described previously (Liu et al., 2008).

ACCESSION NUMBERS

Microarray data can be obtained from NCBI GEO at series accession GSE27660.

SUPPLEMENTAL INFORMATION

Supplemental Information includes Supplemental Experimental Procedures and three figures and can be found with this article online at doi:10.1016/j.chom.2011.02.003.

ACKNOWLEDGMENTS

We thank Paolo Manzanillo and Jeffery S. Cox for the kind gift of bone marrow-derived macrophages. This work was supported by grant R01AI065519 from the National Institute of Allergy and Infectious Disease (NIAID) to H.D.M. C.D.C. and J.C.S.B. are supported by NIAID grant 5T32AI060537-07 to the University of California, San Francisco Microbial Pathogenesis Program.

Received: October 22, 2010
Revised: January 6, 2011
Accepted: February 4, 2011
Published: March 16, 2011

REFERENCES

Blackstock, R., and Murphy, J.W. (1997). Secretion of the C3 component of complement by peritoneal cells cultured with encapsulated Cryptococcus neoformans. Infect. Immun. *65*, 4114–4121.

Botts, M.R., and Hull, C.M. (2010). Dueling in the lung: how Cryptococcus spores race the host for survival. Curr. Opin. Microbiol. *13*, 437–442.

Chow, E.D., Liu, O.W., O'Brien, S., and Madhani, H.D. (2007). Exploration of whole-genome responses of the human AIDS-associated yeast pathogen Cryptococcus neoformans var grubii: nitric oxide stress and body temperature. Curr. Genet. *52*, 137–148.

Chun, C.D., and Madhani, H.D. (2010). Ctr2 links copper homeostasis to polysaccharide capsule formation and phagocytosis inhibition in the human fungal pathogen Cryptococcus neoformans. PLoS ONE *5*, e12503.

Chun, C.D., Liu, O.W., and Madhani, H.D. (2007). A link between virulence and homeostatic responses to hypoxia during infection by the human fungal pathogen Cryptococcus neoformans. PLoS Pathog. *3*, e22.

Datta, K., Bartlett, K.H., Baer, R., Byrnes, E., Galanis, E., Heitman, J., Hoang, L., Leslie, M.J., MacDougall, L., Magill, S.S., et al; Cryptococcus gattii Working Group of the Pacific Northwest. (2009). Spread of Cryptococcus gattii into Pacific Northwest region of the United States. Emerg. Infect. Dis. *15*, 1185–1191.

Del Poeta, M. (2004). Role of phagocytosis in the virulence of Cryptococcus neoformans. Eukaryot. Cell *3*, 1067–1075.

Dromer, F., Aucouturier, P., Clauvel, J.P., Saimot, G., and Yeni, P. (1988). Cryptococcus neoformans antibody levels in patients with AIDS. Scand. J. Infect. Dis. *20*, 283–285.

Dromer, F., Denning, D.W., Stevens, D.A., Noble, S.M., and Hamilton, J.R. (1995). Anti-Cryptococcus neoformans antibodies during cryptococcoss in patients with acquired immunodeficiency syndrome. Serodiagnosis and Immunotherapy in Infectious Disease *7*, 181–188.

Hejgaard, J., Jacobsen, S., Bjørn, S.E., and Kragh, K.M. (1992). Antifungal activity of chitin-binding PR-4 type proteins from barley grain and stressed leaf. FEBS Lett. *307*, 389–392.

Hull, C.M., Cox, G.M., and Heitman, J. (2004). The alpha-specific cell identity factor Sxi1alpha is not required for virulence of Cryptococcus neoformans. Infect. Immun. *72*, 3643–3645.

Jung, W.H., Sham, A., White, R., and Kronstad, J.W. (2006). Iron regulation of the major virulence factors in the AIDS-associated pathogen Cryptococcus neoformans. PLoS Biol. *4*, e410.

Levitz, S.M., and DiBenedetto, D.J. (1989). Paradoxical role of capsule in murine bronchoalveolar macrophage-mediated killing of Cryptococcus neoformans. J. Immunol. *142*, 659–665.

Liu, O.W., Chun, C.D., Chow, E.D., Chen, C., Madhani, H.D., and Noble, S.M. (2008). Systematic genetic analysis of virulence in the human fungal pathogen Cryptococcus neoformans. Cell *135*, 174–188.

Lohse, M.B., and Johnson, A.D. (2008). Differential phagocytosis of white versus opaque Candida albicans by Drosophila and mouse phagocytes. PLoS ONE *3*, e1473.

Luberto, C., Martinez-Mariño, B., Taraskiewicz, D., Bolaños, B., Chitano, P., Toffaletti, D.L., Cox, G.M., Perfect, J.R., Hannun, Y.A., Balish, E., and Del Poeta, M. (2003). Identification of App1 as a regulator of phagocytosis and virulence of Cryptococcus neoformans. J. Clin. Invest. *112*, 1080–1094.

McClelland, C.M., Chang, Y.C., and Kwon-Chung, K.J. (2005). High frequency transformation of Cryptococcus neoformans and Cryptococcus gattii by Agrobacterium tumefaciens. Fungal Genet. Biol. *42*, 904–913.

Monari, C., Bistoni, F., and Vecchiarelli, A. (2006a). Glucuronoxylomannan exhibits potent immunosuppressive properties. FEM. Yeast Res. *6*, 537–542.

Monari, C., Kozel, T.R., Paganelli, F., Pericolini, E., Perito, S., Bistoni, F., Casadevall, A., and Vecchiarelli, A. (2006b). Microbial immune suppression mediated by direct engagement of inhibitory Fc receptor. J. Immunol. *177*, 6842–6851.

Monga, D.P. (1981). Role of macrophages in resistance of mice to experimental cryptococcosis. Infect. Immun. *32*, 975–978.

Nobile, C.J., Nett, J.E., Hernday, A.D., Homann, O.R., Deneault, J.S., Nantel, A., Andes, D.R., Johnson, A.D., and Mitchell, A.P. (2009). Biofilm matrix regulation by Candida albicans Zap1. PLoS Biol. *7*, e1000133.

Nussbaum, G., Anandasabapathy, S., Mukherjee, J., Fan, M., Casadevall, A., and Scharff, M.D. (1999). Molecular and idiotypic analyses of the antibody response to Cryptococcus neoformans glucuronoxylomannan-protein conjugate vaccine in autoimmune and nonautoimmune mice. Infect. Immun. *67*, 4469–4476.

Osterholzer, J.J., Milam, J.E., Chen, G.H., Toews, G.B., Huffnagle, G.B., and Olszewski, M.A. (2009). Role of dendritic cells and alveolar macrophages in regulating early host defense against pulmonary infection with Cryptococcus neoformans. Infect. Immun. *77*, 3749–3758.

Park, B.J., Wannemuehler, K.A., Marston, B.J., Govender, N., Pappas, P.G., and Chiller, T.M. (2009). Estimation of the current global burden of cryptococcal meningitis among persons living with HIV/AIDS. AIDS *23*, 525–530.

Rothman, B.L., Merrow, M., Despins, A., Kennedy, T., and Kreutzer, D.L. (1989). Effect of lipopolysaccharide on C3 and C5 production by human lung cells. J. Immunol. *143*, 196–202.

Subramaniam, K., Metzger, B., Hanau, L.H., Guh, A., Rucker, L., Badri, S., and Pirofski, L.A. (2009). IgM(+) memory B cell expression predicts HIV-associated cryptococcosis status. J. Infect. Dis. *200*, 244–251.

Teakle, G.R., and Gilmartin, P.M. (1998). Two forms of type IV zinc-finger motif and their kingdom-specific distribution between the flora, fauna and fungi. Trends Biochem. Sci. *23*, 100–102.

Tejle, K., Magnusson, K.E., and Rasmusson, B. (2002). Phagocytosis and phagosome maturation are regulated by calcium in J774 macrophages interacting with unopsonized prey. Biosci. Rep. *22*, 529–540.

Torres, H.A., Prieto, V.G., Raad, I.I., and Kontoyiannis, D.P. (2005). Proven pulmonary cryptococcosis due to capsule-deficient Cryptococcus neoformans does not differ clinically from proven pulmonary cryptococcosis due to capsule-intact Cr. neoformans. Mycoses *48*, 21–24.

Tusher, V.G., Tibshirani, R., and Chu, G. (2001). Significance analysis of microarrays applied to the ionizing radiation response. Proc. Natl. Acad. Sci. USA *98*, 5116–5121.

Voelz, K., and May, R.C. (2010). Cryptococcal interactions with the host immune system. Eukaryot. Cell *9*, 835–846.

Cell Host & Microbe, *Volume 9*

Supplemental Information

A Major Role for Capsule-Independent Phagocytosis-Inhibitory Mechanisms in Mammalian Infection by *Cryptococcus neoformans*

Cheryl D. Chun, Jessica C.S. Brown, and Hiten D. Madhani

Supplemental Experimental Procedures

Strains and media

C. neoformans was routinely grown in yeast culture conditions (on YPAD medium [1% yeast extract, 2% Bacto-peptone, 2% glucose, 0.015% L-tryptophan, 0.004% adenine] at 30ºC) or in tissue culture conditions (in Dulbelco's Modified Eagle Medium [DMEM] with 4.5 g/L glucose at 37ºC with 5% CO_2). All strains were constructed by biolistic transformation into the serotype A strain H99. The construction of strains *gat201*Δ-1 and *gat201*Δ-2 was previously described (Liu et al., 2008). Gat201-CBP-2X FLAG was generated by the insertion of the epitope CBP-2XFLAG at the 3' end of the endogenous *GAT201* gene, marked with a NAT resistance cassette at the 3' end of the transformation construct. Phagocytosis measurements demonstrated that this tag did not block the function of Gat201 (C.D.C. and H.D.M., unpublished observations). *gat204*Δ was constructed by disrupting the GATA-domain of *CNAG_06762* with a NAT resistance cassette. *blp1*Δ was constructed by disrupting the entire coding sequence of *CNAG_06346* with a NAT resistance cassette. *blp1*Δ*gat204*Δ was constructed by disrupting the entire coding sequence of *CNAG_06346* with a NEO resistance cassette in the *gat204*Δ strain. *gat204*Δ *blp1*Δ was constructed by disrupting the entire coding sequence of *CNAG_06762* with a NEO resistance cassette in the *blp1*Δ strain. Strains used in this study are listed in Table 1.

Phagocytois assays

RAW264.7 macrophages ($2x10^4$ cells/well) were seeded into 96-well tissue-culture treated plates in DMEM medium and allowed to adhere overnight. *C. neoformans* cells grown in YPAD medium were washed three times with PBS then resuspended to a density of $5x10^6$ cells/ml in PBS, and 10 μl ($5x10^4$ cells) were co-incubated with the RAW264.7 macrophages in 200 μl fresh DMEM. Following 24 hours co-incubation, the macrophages were washed three times with PBS to remove unphagocytosed yeast, then fixed with 1% formaldehyde/PBS prior to visualization on an inverted light microscope. Percentage of yeast cell-associated macrophages was determined by counting the number of macrophages with yeast internalized or associated with their cell surface, divided by the number of macrophages counted. At least 200 macrophages were assayed per well, and each strain was tested in triplicate.

For measuring the internalization of yeast cells by macrophages, phagocytosis assays were performed as described above, except $3x10^4$ cells were plated per well and the number of *C. neoformans* cells added per well were adjusted accordingly (to $7.5x10^4$ cells). Following co-incubation and fixation, wells were washing once in PBS and

percentage of yeast cell-associated macrophages determined as described above ("pre-wash" data in Figure S3). Wells were then washed two more times in PBS and incubated overnight at 4°C in PBS + mouse anti-GXM (1:1000) + mouse anti-β-glucan (1:1000) antibodies. Wells were washed another two times in PBS, incubated 1hr in PBS + FITC-conjugated anti-mouse secondary antibody (1:1000), washed three times in PBS, then incubated 30 minutes in PBS + 0.5% SDS to permeabilize macrophages. Wells were washed three times in PBS, then incubated overnight at 4°C in PBS + 0.1% Triton-X 100 + mouse anti-GXM (1:1000) antibody. Wells were washed twice in PBS, incubated 1hr in PBS + 0.1% Triton-X 100 + TRITC-conjugated anti-mouse secondary antibody (1:1000), then washed a final time in PBS. Percentage of yeast-associated macrophages was determined as described above. Whether said yeast cells were internalized (TRITC staining only) or externally associated (FITC and TRITC staining) was determined for each strain background. 10 yeast-associated macrophages were analyzed per well for wild type and *blp1*Δ strains and 30 yeast-associated macrophages were analyzed per well for *gat201*Δ, *gat204*Δ, and *gat204*Δ*blp1*Δ strains. Three wells were analyzed for each strain. Microscopy was performed on an Axiovert 200M (Zeiss) microscope running Axiovision software.

Bone marrow-derived macrophage (BMDM) phagocytosis assays were performed as described for RAW264.7 cells, excepting that BMDMs were fixed in 4% paraformaldehyde (in PBS) instead of 1% formaldehyde. BMDM cells were a gift from Paolo Manzanillo and Jeffrey Cox and were isolated as described in Shiloh et al., 2008 (Shiloh et al., 2008).

Expression profiling

Three or eight replicate cultures each of H99 and *gat201*Δ were grown overnight to saturation in YPAD at 30°C. For microarrays grown in YPAD medium, cultures were diluted to an OD_{600} of 0.1 in YPAD, grown at 30°C to $OD6_{00}$ = 1.0, and then harvested by centrifugation and snap freezing. For samples grown in DMEM, the volume of YPAD-grown culture equivalent to OD_{600} = 50 was washed three times with PBS prior to resuspension in 20 ml DMEM. The cultures were incubated for 24 hours in 15 cm tissue culture-treated dishes (Corning) at 37ºC with 5% CO_2. The cultures were harvested by centrifugation and snap freezing. RNA isolation, array hybridizations, and data analysis using SAM analysis were performed as described previously (Chun et al., 2007). Shown are the genes that have at least a two-fold average difference in gene expression between wild type and mutant following SAM analysis of the arrays from tissue-culture conditions.

ChIP-on-chip

The ChIP-chip tiling arrays were designed on 244,000 probes of 60-bp length, averaging 80-bp between probes, across the entire H99 sequence as it was published by the Broad Institute, current to 2007. *C. neoformans* strains were grown overnight to saturation in YPAD at 30°C. The equivalent volume of OD_{600} = 200 were washed three times with PBS prior to resuspension in 80 ml DMEM. The cultures split between four 15 cm tissue culture-treated dishes (Corning) and incubated for 8 hours at 37°C with 5% CO_2. The cultures were fixed with 1% formaldehyde, followed by quenching with 125 mM glycine, then harvested by centrifugation and snap freezing. Samples were lyophilized, and chromatin immunoprecipitation performed as previously described (Nobile et al., 2009) with the following minor modifications: zirconia/silica beads (0.5 mm diameter) were used to lyse the cells via a Bead Beater-8, used for thirty minutes with frequent rests on ice. The chromatin in the cell pellet was sonicated for 1 hr in a Diagenode

Bioruptor (settings: 4x15 min, 30 s on, 1 min off) at 4ºC. Immunoprecipitation was performed with an anti-FLAG antibody. Following ChIP, strand displacement amplification and labeling were performed as previously described to generate DNA probes with incorporated aminoallyl-dUTP which were then hybridized as described to the tiling arrays (Nobile et al., 2009). Analysis was performed by calculating the median of the top five probes in the 2kb flanking the start codon of each gene. The median value for the untagged strain was subtracted from the median value of the tagged strain, yielding the difference for the pair of untagged/tagged arrays. The calculation was repeated for a second duplicate pair of untagged/tagged arrays. The calculated differences were clustered using the software Cluster, and the cluster showing increased binding in both pairs was isolated for additional analysis. In this cluster, the differences were averaged between the two pairs, and the genes with greater than 1.9-fold median enrichment in tagged versus untagged arrays were selected for screening for Gat201-dependent gene expression by RT-qPCR. Phagocytosis measurements demonstrated that the tag did not block the function of Gat201 (C.D.C. and H.D.M., unpublished observations).

Binding Motif Analysis

A putative binding motif for Gat201 was identified using MochiView software v.1.37 (http://johnsonlab.ucsf.edu/sj/mochiview-software/) (Homann and Johnson, 2010). 1 kb of sequence upstream of the start codon of each gene was isolated and used as a reference set, with which to compare the 1 kb sequences upstream from the start codon of the 62 genes transcriptionally-induced by Gat201. The Motif Finder feature of MochiView was used for this analysis, and identified the seven bp putative binding motif.

RT-qPCR

Gene expression differences observed using microarray-based transcript profiling were confirmed utilizing RT-qPCR. cDNA was synthesized using Superscript III Reverse Transcriptase (Invitrogen) and oligo-DT and random nonamer primers. Approximately 0.2 ng of cDNA was used as template in a qPCR reaction containing SYBR Green dye (Molecular Probes). Fluorescent signal was measured on an Opticon DNA Engine PCR machine (MJ Research). For each primer set, standard curves were generated using 5-fold serial dilutions of cDNA to account for differences in priming efficiencies. For each sample, values were normalized to the levels of actin (ACT1). MEU1 (CNAG_00165) qPCR primers were C1550/C1551. CNJ1810 (CNAG_04735) qPCR primers were C1554/C1555. *GAT204* qPCR primers were C2416/C2417. *BLP1* qPCR primers were: AAG AGG ATC ACC CAC AC TGG and ATC ATT GCA ACC AGG ACA CA.

A. tumefaciens*-mediated transformation of *C. neoformans

Transformation was carried out as in McClelland et al (2005) with minor changes: prior to mixing strain C601 with H99, the OD600 of C601 was adjusted to 0.5 and H99 was adjusted to 5.85. Equal aliquots of C601 and H99 were mixed together. 400 µl of C601+H99 were plated onto 0.45 um Biodyne® A membranes (PALL Life Sciences, Cat. no. 601012) placed on induction medium agar plates containing 200 µM acetosyringone. The plates were incubated at 25°C for 3 days. The membranes were then transferred to YPAD plates containing 0.1 mg/ml norseothrycin and 200 µM cefotaxime. These plates were then incubated at 30°C for two days until *C. neoformans* growth was seen. The membranes were then washed with PBS to remove the *C. neoformans* cells and the cells from all membranes were pooled together. The resulting

library was washed three times with PBS, before being frozen down in 15% glycerol. We estimated ~30,000 transformants were generated in this library.

Phagocytosis Screen with Insertional Mutant Library

$2x10^7$ RAW264.7 macrophages were seeded into 15 cm tissue culture dishes (Corning) in 20 ml DMEM medium and allowed to adhere overnight. *C. neoformans* cells from overnight cultures grown in YPAD medium with 200 µm cefotaxime were washed three times with PBS then added to the RAW264.7 macrophages in 20 ml fresh DMEM at an MOI of 10:1. Following 24 hours co-incubation, the macrophages were washed three times with PBS to remove unphagocytosed yeast, then lysed with 0.01% SDS. Cell lysis was confirmed visually on a light microscope. The lysed cells were collected and washed three times in PBS prior to resuspension in YPAD medium with 200 µM cefotaxime. The harvested yeast were then plated on YPAD agar plates containing nourseothricin and 200µM cefotaxime. Colonies that grew up were picked and individually assayed for rates of phagocytosis.

Capsule assay

C. neoformans strains were grown in YPAD overnight to saturation. $2x10^7$ cells were washed three times in PBS prior to resuspension in 2.5 ml DMEM. Cultures were incubated in 6-well tissue culture-treated dishes (BD Biosciences) for 24 hours at 37ºC with 5% CO_2. The cells were collected, fixed with 1% formaldehyde, and washed twice with PBS. The cells were incubated for 1 hour at 37ºC with a previously described mouse monoclonal antibody (mAB339) specific for the main capsule polysaccharide glucoronoxylomannan (Belay et al., 1997). The cells were then washed twice with PBS, prior to incubation with FITC-conjugated donkey anti-mouse antibody (Jackson ImmunoResearch) for 1 hour at room temperature in the dark. The cells were then washed twice with PBS, and 4 µL of India ink was added to 20 µL of sample. The capsule was visualized at 63x magnification using an Axiovert 200M (Zeiss) microscope running Axiovision software. To quantify capsule size, the cell diameter and capsule diameter of at least 30 cells per strain were measured.

Intranasal co-infection experiments.

C. neoformans strains were individually grown in liquid YPD cultures overnight at 30°C. Cells were washed twice in PBS then counted using a hemacytometer and an equal number of WT cells and cells of the co-infecting strain were combined to a final concentration of 1×10^7 cells/ml. 6 week-old female A/J (NCI) mice were anesthetized by intraperitoneal injection of ketamine (75 mg/kg) and medetomidine (0.5-1.0 mg/kg). The mice were then suspended from a silk thread by their front incisors and 50µl of the inoculum (5×10^5 cells) were slowly pipetted into the nares. After 10 minutes, the mice were lowered and the anesthesia was reversed by intraperitoneal injection of atiplamezole (1.0-2.5 mg/kg). Three mice were infected per inoculum. A dilution of each inoculum was also plated on Sabouraud agar plates containing 40 mg/ml gentamicin and 50 mg/ml carbenicillin. The plates were incubated for two days at 30°C, colonies were counted to verify the concentration of cells in the inoculum, and the proportion of mutant cells in the inoculum was determined by assaying 100-200 colonies for NAT resistance on YPD agar plates containing 100mg/ml NAT. Mice were sacrificed by CO_2 inhalation followed by cervical dislocation three days post-infection and the lungs were removed and homogenized in 5 ml sterile PBS. Serial dilutions of each organ sample were plated on Sabouraud agar plates containing 40 mg/ml gentamicin and 50 mg/ml carbenicillin. The plates were incubated for two days at 30°C, colonies were isolated, and the

proportion of mutant cells within each organ was determined by assaying 100-200 colonies for NAT resistance on YPD agar plates containing 100mg/ml NAT.

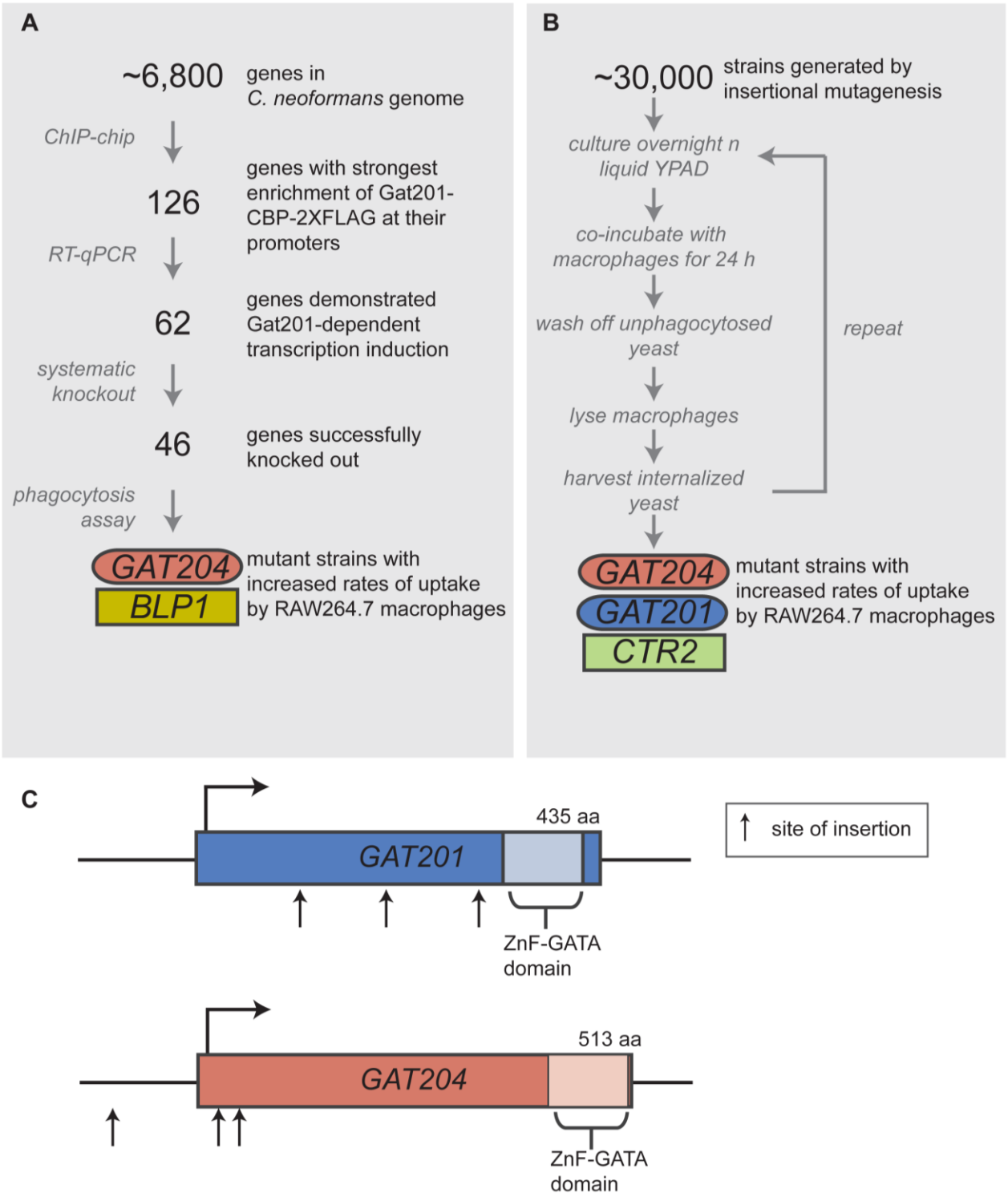

Figure S1. Two Redundant Approaches to Identify Genes Required for Anti-Phagocytosis, Related to Figure 2

(A) Approach 1. 126 genes with the strongest enrichment of Gat201-CBP-2XFLAG in their promoter regions were assayed by RT-qPCR in WT and *gat201*Δ strains. 62 genes showed Gat201-dependent transcription induction. Of these, 46 genes were knocked out

and screened in a phagocytosis assay. Two strains, mutated in *GAT204* and *BLP1*, showed increased uptake by macrophages.
(B) Approach 2. Approximately 30,000 mutant *C. neoformans* strains were generated by insertional mutagenesis. These strains were co-incubated with macrophages or 24 hours prior to removal of unphagocytosed yeast by PBS washes. The internalized yeast strains were harvested from lysed macrophages and re-assayed by phagocytosis assay. Mutations in three genes were identified: *GAT204*, *GAT201* and *CTR2*.
(C) Sites of insertion of NAT^R cassette into the genes *GAT201* and *GAT204* in mutant strains identified in the screen described in (B).

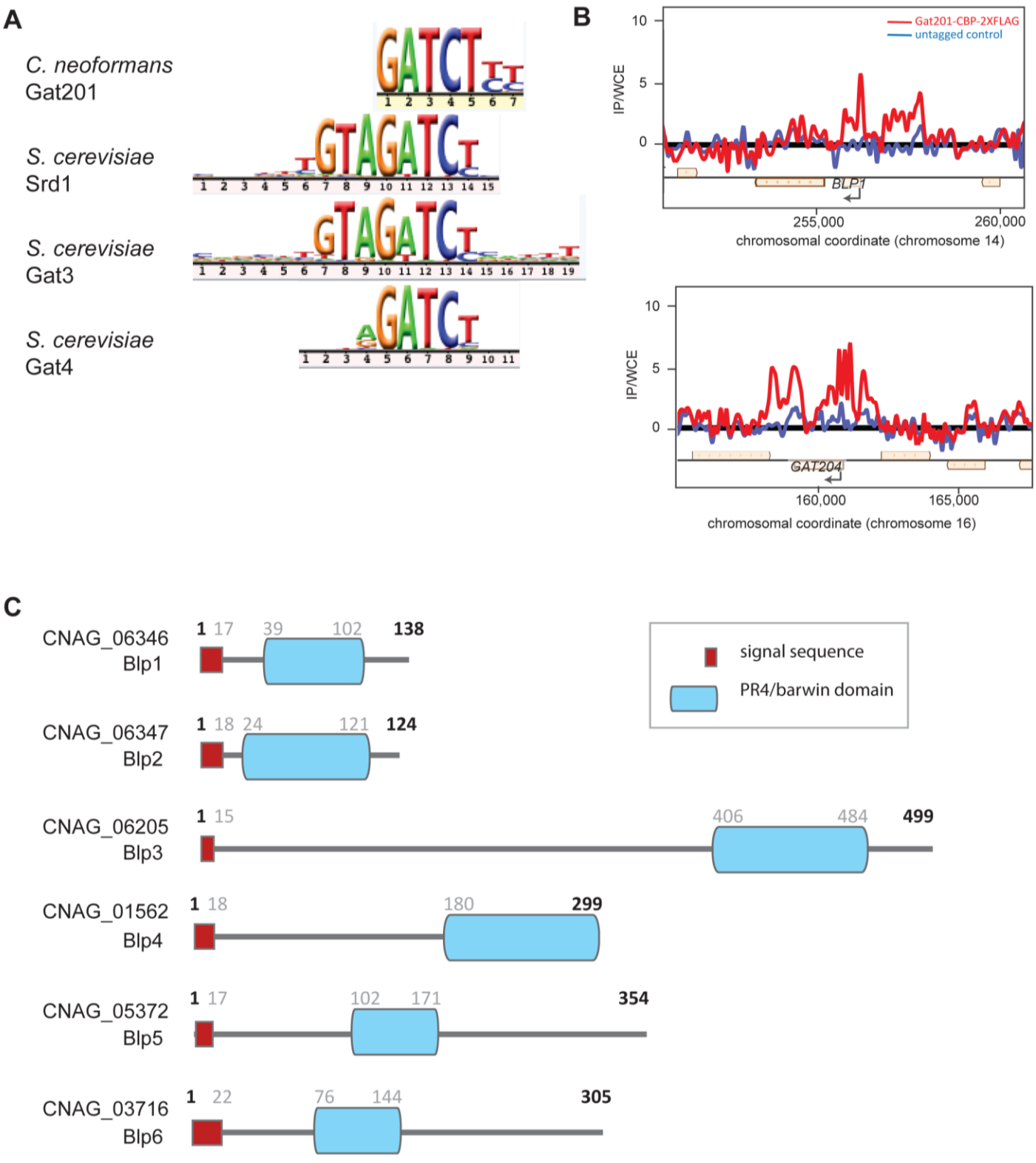

Figure S2. Features of Gat201 Targets, Related to Figure 1

(A) A distinct motif is enriched in the promoters of Gat201-bound genes. A motif-finding algorithm in the MochiView package identified a motif enriched in the promoters of

Gat201-bound genes when compared to the overall sequence of the genome. The motif shows striking similarity to already characterized binding sequences of *S. cerevisiae* GATA-family transcription factors Srd1, Gat3 and Gat4 (Badis et al., 2008).
(B) Gat201-CBP-2xFLAG binds in the promoter regions of *BLP1* and *GAT204*. Ratio of immunoprecipitated DNA (IP) to whole cell extract (WCE) plotted for each probe of the two tiling arrays at the chromosomal coordinates indicated.
(C) Schematic of Blp1 and its five family members. Blp1 is a 138 amino acid protein predicted by SMART protein analysis to have a Barwin-like domain (residues 39-102). SignalP analysis predicts a signal sequence in the first 17 residues with a probability of 1.000. Blp1 is a member of a six-protein family, all of which contain a Barwin-like domain and a signal sequence (as predicted by SignalP). We have named these genes *BLP2-6*. *BLP1* is the only gene in this family whose mRNA is induced by Gat201, as determined by RT-qPCR (C.D.C and H.D.M., unpublished observations). Error bars indicate SD.

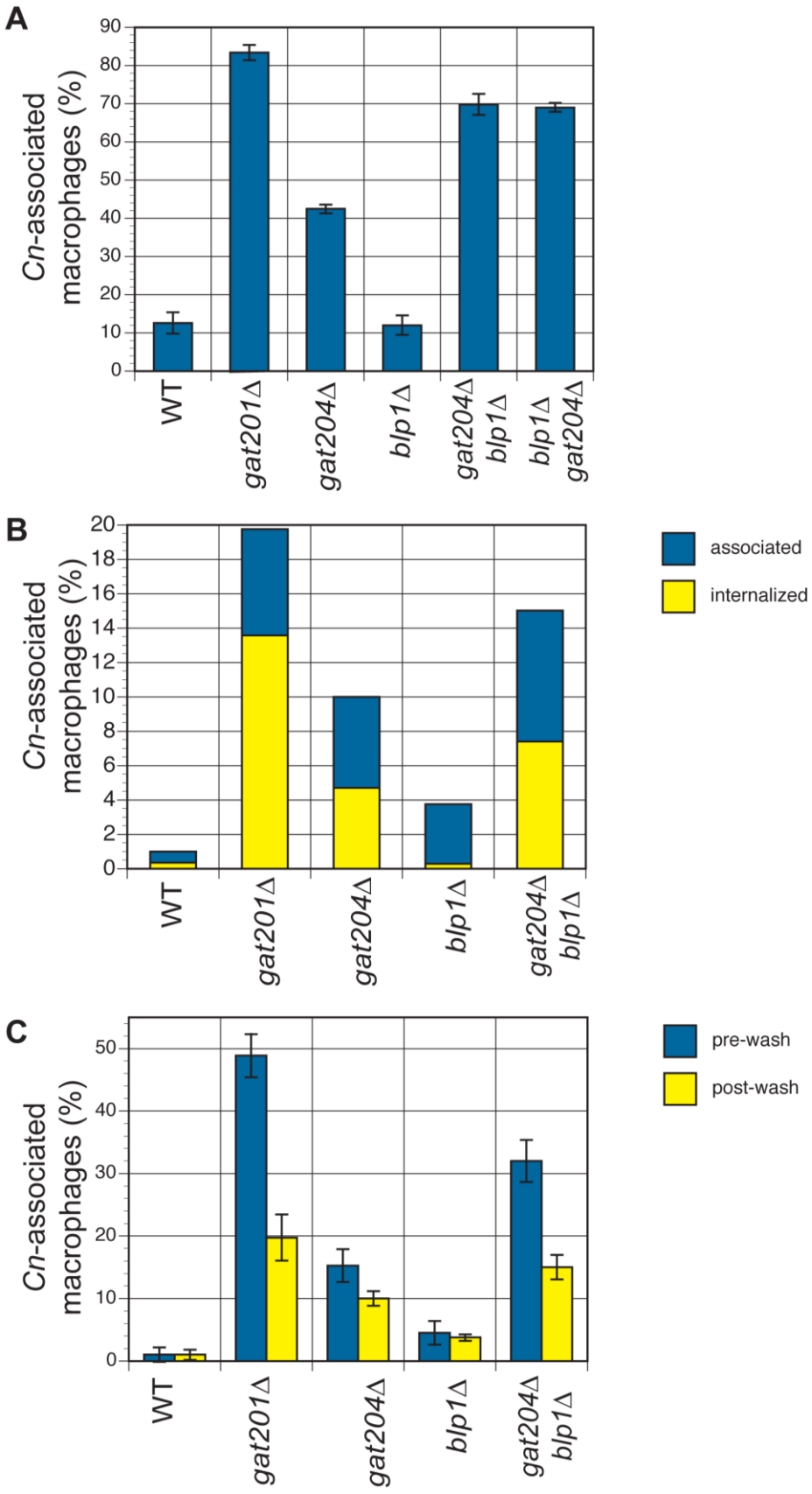
A
Cn-associated macrophages (%)
0
10
20
30
40
50
60
70
80
90
WT
gat201Δ
gat204Δ
blp1Δ
gat204Δ blp1Δ
blp1Δ gat204Δ
B
Cn-associated macrophages (%)
0
2
4
6
8
10
12
14
16
18
20
WT
gat201Δ
gat204Δ
blp1Δ
gat204Δ blp1Δ
associated
internalized
C
Cn-associated macrophages (%)
0
10
20
30
40
50
WT
gat201Δ
gat204Δ
blp1Δ
gat204Δ blp1Δ
pre-wash
post-wash

Figure S3. Additional Phagocytosis Experiments, Related to Figure 3
(A) Quantification of phagocytosis defects. Bone marrow-derived macrophages from C57/Bl6 mice (a gift from P. Manzanillo and J. Cox) were co-incubated with the designated *C. neoformans* strains for 24 hours, then washed three times with PBS to remove unphagocytosed yeast. The macrophages were then counted to assay the number of macrophages with yeast associated. At least 100 macrophages were counted per well and each strain was assayed in triplicate. Error bars indicate SD.
(B) Differential staining of *C. neoformans* to distinguish yeast internalized by macrophages from those only associated externally. Phagocytosis assays were performed as described above using RAW264.7 cells. Unassociated yeast cells were removed by washing three times in PBS. Samples were then fixed in 4% paraformaldehyde, washed, then yeast cells labeled with anti-GXM and anti-β-glucan antibodies, followed by a FITC-conjugated secondary antibody, to label accessible (externally-associated) yeast cells. Samples were washing again, the macrophages permeabilized in PBS containing 0.5% SDS, and then treated again with anti-GXM antibody and TRITC-conjugated secondary antibody (to label yeast internalized by macrophages). The overage percentage of macrophages with associated yeast were determined, then the percentage of those macrophages that had either only externally associated yeast (FITC-stained; yellow bars) or contained at least one yeast cell that was completely internalized (TRITC-staining only, blue bars; note: most macrophages with associated yeast cells are associated with multiple yeast cells). At least 100 macrophages were counted per well and each strain assayed in triplicate when determining the overall percentage of macrophages with associated yeast. A minimum of 30 (*gat201*Δ, *gat204*Δ, and *gat204*Δ*blp1*Δ strains) or 10 (wild type and *blp1*Δ strains) macrophages with associated yeast were analyzed per well to determine percent macrophages with internalized yeast versus percent with only externally-associated yeast. *gat201*Δ, *gat204*Δ, and *gat204*Δ*blp1*Δ cells all show an increase in the percentage of macrophages with internalized yeast cells, demonstrating that Gat204 and Gat204 and Blp1 together block phagocytosis of *C. neoformans* by macrophages and not just external association with macrophages.
(C) Percent of macrophages with associated yeast was determined after fixation in paraformaldehyde (pre-wash, blue bars) and after the staining and washing procedure described in part A (post-wash, yellow bars). Both macrophages and yeast cells are lost during the numerous washes of the staining procedure, but the trends remain the same. Specifically, *gat201*Δ cells show the greatest percentage of macrophages with associated yeast both pre- and post-washing and *gat204*Δ*blp1*Δ shows a significant increase in yeast-associated macrophages both pre- and post-washing compared to *gat204*Δ (Student's t-test, $p = 3.9 \times 10^{-3}$). Error bars indicate SD.

Supplemental References

Badis, G., Chan, E.T., van Bakel, H., Pena-Castillo, L., Tillo, D., Tsui, K., Carlson, C.D., Gossett, A.J., Hasinoff, M.J., Warren, C.L.*, et al.* (2008). A library of yeast transcription factor motifs reveals a widespread function for Rsc3 in targeting nucleosome exclusion at promoters. Mol Cell *32*, 878-887.

Belay, T., Cherniak, R., Kozel, T.R., and Casadevall, A. (1997). Reactivity patterns and epitope specificities of anti-Cryptococcus neoformans monoclonal antibodies by enzyme-linked immunosorbent assay and dot enzyme assay. Infect Immun *65*, 718-728.

Chun, C.D., Liu, O.W., and Madhani, H.D. (2007). A link between virulence and homeostatic responses to hypoxia during infection by the human fungal pathogen Cryptococcus neoformans. PLoS Pathog *3*, e22.

Homann, O., and Johnson, A. (2010). MochiView: versatile software for genome browsing and DNA motif analysis. BMC Biology *8*, 49.

Liu, O.W., Chun, C.D., Chow, E.D., Chen, C., Madhani, H.D., and Noble, S.M. (2008). Systematic genetic analysis of virulence in the human fungal pathogen Cryptococcus neoformans. Cell *135*, 174-188.

Nobile, C.J., Nett, J.E., Hernday, A.D., Homann, O.R., Deneault, J.S., Nantel, A., Andes, D.R., Johnson, A.D., and Mitchell, A.P. (2009). Biofilm matrix regulation by Candida albicans Zap1. PLoS Biol *7*, e1000133.

Shiloh, M.U., Manzanillo, P., and Cox, J.S. (2008). Mycobacterium tuberculosis Senses Host-Derived Carbon Monoxide during Macrophage Infection. Cell Host Microbe *3*, 323-330.